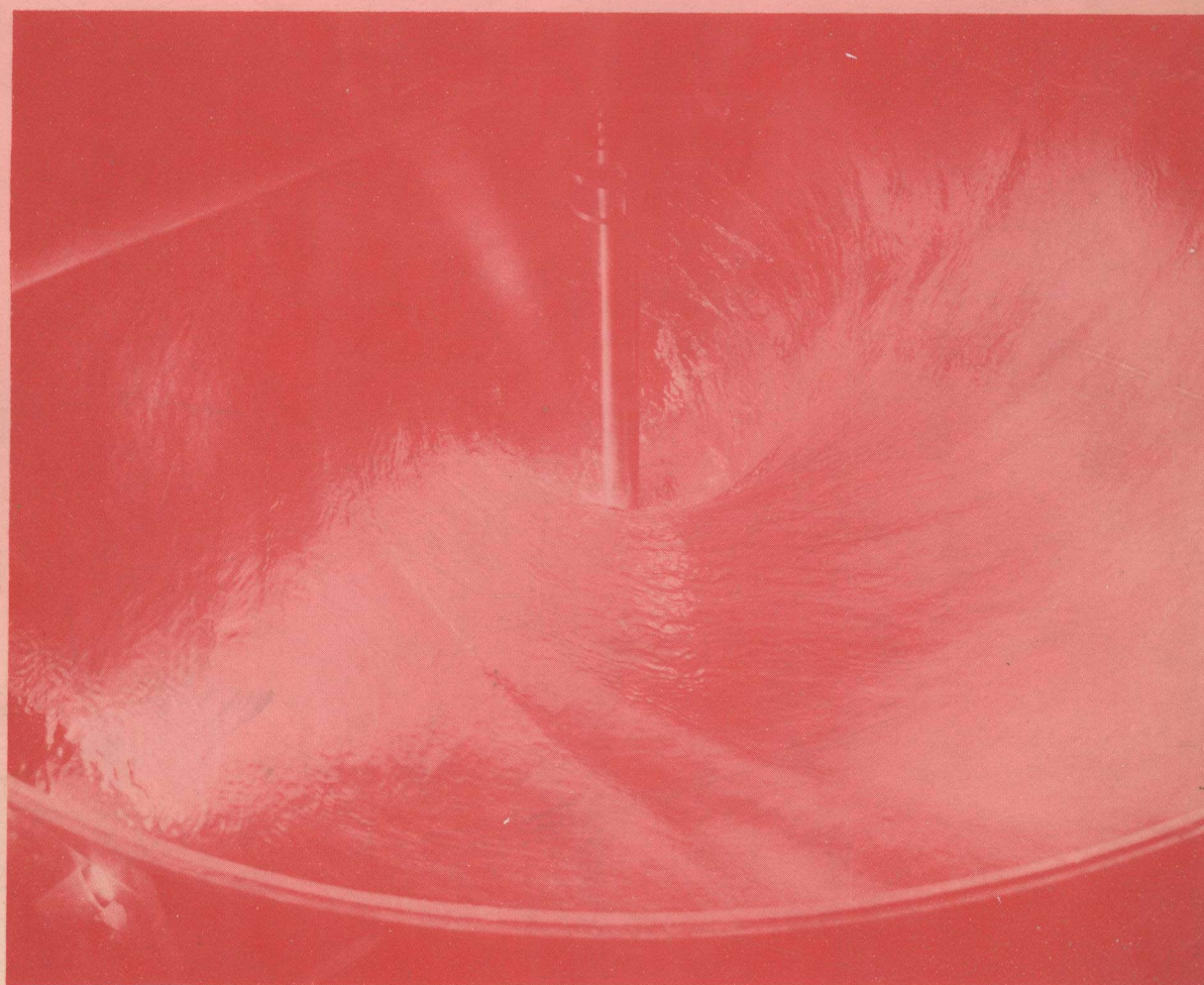


**Proceedings of the
Third European Conference
on
MIXING**

York, England. April, 1979

Volume 1



**Proceedings of the
Third European Conference
on
MIXING**

**HELD AT THE
UNIVERSITY OF YORK, ENGLAND**

APRIL 4th - 6th, 1979

Volume 1

**Organised by BHRA Fluid Engineering
in conjunction with the Institution of Chemical Engineers**



Editors: H.S. Stephens
Mrs. C.A. Stapleton

Volume 1 contains 23 of the papers presented at the 3rd European Conference on Mixing. The remaining papers and an edited record of the discussion and contributions to these papers will appear in Volume 2.

The Organisers are not responsible for statements or opinions made in the papers or in the discussion and contributions.

These papers have been reproduced by offset printing from the authors' original typescript to minimise delay.



British Library Cataloguing in Publication Data

European Conference on Mixing, 3rd, York, 1979
Proceedings of the 3rd European Conference
on Mixing.
I. Mixing - Congresses
I. Stephens, Herbert Simon
II. Stapleton, Christine A
III. British Hydromechanics Research Association
660.2'84292 TP156.M5

ISBN 0-906085-31-4

Printed and Published by:

BHRA Fluid Engineering
Cranfield, Bedford, MK43 0AJ, England.

© BHRA Fluid Engineering, Copyright 1979.

Set of 2 Vols: ISBN 0 906085 31 4
Vol. 1 ISBN 0 906085 32 2
Vol. 2 ISBN 0 906085 33 0

ACKNOWLEDGEMENTS

The valuable assistance of the Organising Committee and Panel of Referees is gratefully acknowledged.

ORGANISING COMMITTEE

Dr. C. Schofield (Chairman)	Warren Spring Laboratory
Dr. M.F. Edwards	University of Bradford
Dr. R. King	BHRA Fluid Engineering
Dr. J.C. Middleton	ICI Corporate Laboratory
Dr. A. Nienow	University College, London
Mr. H.S. Stephens	BHRA Fluid Engineering
Mrs. C.A. Stapleton (Secretary)	BHRA Fluid Engineering

CITATION

When citing papers from this volume, the following reference should be used:-

Title, Author, Proc. 3rd European Conference on Mixing,
BHRA Fluid Engineering, Cranfield, Bedford, England.
Volume 1, Paper No., Pages. (April, 1979).

Third European Conference on Mixing
York, England. : April 4th-6th, 1979

CONTENTS
(Volume 1)

The following papers were presented:

Paper:	Page
A1 Batch and continuous blending of Newtonian fluids using helical ribbon impellers. J.R. Bourne, E.T.H. Zurich, Switzerland, W. Knoepfli, Escher Wyss AG, Switzerland and R. Riesen, Mettler Instrumente AG, Switzerland.	1
A2 Measurement of circulation within large mixing vessels. J.C. Middleton, ICI Corporate Laboratory, U.K.	15
A3 Liquid-liquid mixing in tanks and reservoirs. K.H.M. Ali and R.B. Whittington, University of Liverpool, U.K.	37
A4 Some measurements of micromixing in commercial-scale stirred reactors. W. Angst, J.R. Bourne and F. Kozicki, E.T.H. Zurich Switzerland.	61
A5 The role of extensional flows in fluid mixing and dispersion. D.C.-H. Cheng, Warren Spring Laboratory, U.K.	73
A6 Diffusion effects in non-Newtonian mixing. S.H. El Khadem and D.W. Hubbard, Michigan Technological University, U.S.A.	105
A7 Gas mixing in jet-stirred reactors with short residence times. R. David, J.L. Houzelot and J. Villermaux, Laboratoire des Sciences du Genie Chimique, CNRS-ENSIC, France.	113
B1 Solids mixing and segregation in spouted beds. G.S. McNab and J. Bridgwater, Oxford University, U.K.	125
B2 Continuous powder mixing - ribbon blade mixer with free flowing powders. C. Schofield and D.J. Tookey, Warren Spring Laboratory, U.K.	141
C1 Characteristics of agitated tanks in relation to suspension polymerisation. J.C. Lee and P. Tasakorn, University College of Swansea, U.K.	157

Paper

Page

C2	Adapted motionless mixer design. F.A. Streiff, Sulzer Brothers Limited, Switzerland.	171
✓ C3	Hold-up characteristics in continuous liquid-liquid mixers. J. Godfrey, University of Bradford, U.K. and V. Grilo, University of Ljubljana, Yugoslavia.	189
✓ D1	△ The behaviour of mono-size particle slurries in a fully baffled turbulent mixer. R.A. Herringe, M.D. Research Co. Pty. Ltd., Australia	199
D2	225 Solid-liquid mass transfer in stirred vessels. S. Sicardi, R. Conti, G. Baldi and R. Cresta, Turin Polytechnic, Italy.	217
D3	225 Three phase suspensions in agitated vessels. S. Subbarao and V.K. Taneja, Indian Institute of Technology, New Delhi, India.	229
E1	✓ Hydraulic forces on different impeller-types. K.D. Kipke, Ekato Mixing Technology Ltd., U.K.	241
✓ E2	Drop break-up by gas streams. M. Sarjeant, Central Electricity Generating Board, U.K.	255
E3	Safety in mixing operations - a brief review. D.J. Tookey, Warren Spring Laboratory, U.K.	269
F1	✓ The effect of contaminants on the oxygen transfer rate achieved with a plunging jet contractor. J.A.C. Van De Donk, J.M. Smith and R.G.J.M. Van der Lans, T.H. Delft, Netherlands.	289
F2	Mixing and phase distributions in two and three-phase bubble column reactors. M.E. Abou-El-Hassan, Cairo University, Egypt.	303
✓ F3	✓ Circulation rates in stirred and aerated tanks. J. Bryant and S. Sadeghzadeh, University of Exeter, U.K.	325
F4	✓ The chemical method for the determination of the mass transfer in gas-liquid noncoalescent dispersion in agitated reactors: limits of validity and scale up of the experimental data. N. Midoux and J.C. Charpentier, Laboratoire des Sciences du Genie Chimique-ENSIC, France.	337
✓ F5	225 Gas-liquid mixing dynamics in a stirred vessel. M. Greaves and C.A. Economides, University of Bath, U.K.	357

**BATCH AND CONTINUOUS BLENDING OF NEWTONIAN FLUIDS
USING HELICAL RIBBON IMPELLERS**

J.R. Bourne., *W. Knoepfli and **R. Riesen

E.T.H. Zurich, Switzerland

Summary

The helical ribbon impeller has often been recommended for homogenising highly viscous fluids in the laminar flow regime. The first phase of the present investigation covered batch homogenisation at two scales, using 8 helical ribbons having 3 pitches and various wall clearances. The power consumption and the mixing time (measured by an acid/base neutralisation) were measured as functions of stirrer speed and viscosity in glycerine solutions within the laminar and transitional flow regimes. The results were interpreted with respect to:

- a) Scale-up criteria;
- b) The pitch and wall clearance of the helical ribbon, which consumes the least energy when blending Newtonian fluids.

In the second phase the residence time distribution was used to characterise continuous operation, whereby the optimal impeller see b) above was employed. A photo-chromic dyestuff in glycerine was injected into the feed and the outlet concentration represented in the time and the frequency domains. These measurements were used to determine break-through, circulation and mean residence times and also the pumping capacity of the impeller. Downwards pumping avoids quasi-dead zones in secondary circulation loops. In batch and continuous operation with downwards-pumping, three circulations of the tank contents gave a high degree of blending, irrespective of viscosity.

NOMENCLATURE

c	Clearance between helix and tank wall
d	Diameter of helical ribbon
D	Inner diameter of tank
h	Height of helix
K	d/D
N	Rotational speed of helix
P	Power consumption
q	Throughput
Q	Circulation rate
S	Pitch of a helix flight
t_D, t_c, t_m, \bar{t}	Breakthrough, circulation, mixing and mean residence times
w	Width of the helix
V	Liquid volume
z_o	Liquid height with impeller at rest
ρ	Fluid density
μ	Viscosity
τ	Nominal mean residence time (V/q)
Ω	Angular velocity of impeller
ω	Angular velocity of fluid
Po	Power number ($P/\rho N^3 d^5$)
Re	Reynolds number ($N d^2 \rho/\mu$)

INTRODUCTION

Starting with the investigations of Nagata et al. in 1957 (Ref.1), various studies of the flow pattern, power consumption and blending time characteristics of the helical ribbon impeller have shown that the whole fluid is set in motion at a moderate specific power consumption. However a turbine may well produce only local agitation in highly viscous fluids, particularly when they possess pseudoplastic or plastic flow properties (Ref.2). The helix conveys fluid up or down near the wall depending upon its direction of rotation and this fluid circulates and returns via the central region. This primary flow pattern is supplemented by a secondary flow inwards along the base when pumping upwards (Ref.3). For blending highly viscous, Newtonian liquids, the following helix geometry has recently been proposed (Ref.4):

$$s/d = 1 \qquad w/D = 0.1 \qquad d/D = 0.95$$

The first objective of this communication is to present a different optimal geometry, which minimises the energy input for a given mixing time and so limits viscous heating.

Few measurements of the residence time distribution when blending viscous fluids continuously have been published. Only one partial study of the helical ribbon could be found (Ref.5). Among the still open questions are:

- a) A convenient and accurate method to measure the residence time distribution (RTD);
- b) The influence of the feed and offtake points on the blending;
- c) The extent to which correlations (e.g. for circulation time and capacity) obtained in batch experiments are applicable to continuous blending.

The second objective of this paper is to attempt to clarify these matters, at least for viscous Newtonian fluids.

EXPERIMENTAL

Batch operation

Seven helical ribbons having 3 different pitches and 4 different wall clearances, were used in batch experiments at the 0.023 m³ scale (tank diameter 0.29 m). The geometry of the tank/impeller system is shown in Fig.1; the dimensions are given in Table 1, which also includes data for the 0.73 m³ tank (diameter 0.92 m). The linear scale-up factor was 3.17. As indicated in Fig.1, all helices had two flights.

The fluids used were glycerine/water solutions containing up to 10 % water and having densities and viscosities in the ranges 1244-1270 kg m⁻³ respectively 0.18-2.13 Pa s (284-298 K). A N₂ atmosphere was used to avoid absorption of water from the atmosphere and consequent fall in viscosity.

The rotational speed was continuously variable from 3 to 110 rpm in both directions, so changing the pumping direction of the helix. The power absorption was determined from the speed and the couple in the shaft, which was measured by a torque transducer, as explained elsewhere (Ref.6).

The blending time was determined by adding a small quantity of 2N H₂SO₄ solution in glycerine to the tank, which had been made alkaline with NaOH and contained phenolphthalein (pK-value for change from red to colourless = 8.4). Three decolourisations were made for each set of conditions (viscosity, stirrer speed and direction), the times differing by less than 5 % from each other. A total of 24 such measurements were possible before the fluid in the tank had to be changed. The blending time determined by chemical decolourisation depends also on the stoichiometric ratio of acid to base (Ref.7). Typical results are shown in Table 2, here for N = 60 rpm.

The acid/base ratio was standardised at 1.4. The position on the surface at which the acid was added had no effect on the blending time (Ref.8).

Continuous operation

The RTD was measured by introducing a quantity of a photochromic dye into the feed to the tank and measuring its concentration photometrically in the outflow. The dye was then converted to a non-absorbing form before the whole stream was recycled to the mixer. Full details of the experimental technique are given elsewhere (Ref. 9, 10).

The helix used was similar to impeller D (Table 1), having $d/D = 0.91$; $s/d = 0.57$; $h/d = 1.17$; $w/d = 0.12$ and $z_0/d = 1.36$ ($D = 0.290$ m). The volume of liquid in the tank was 0.0234 m^3 . The outlet was directly below the shaft. The inlet, a hole of 0.025 m diameter, was in the tank wall, 0.080 m above the base. $3.5 \times 10^{-5} \text{ m}^3$ of a concentrated dye solution was introduced into the feed without impulse, as explained elsewhere (Ref.9). The inlet signal was approximately a square wave having a width of $2-3$ s or at most 1% of the mean residence time. Sulzer static mixing elements were inserted in the inlet pipe and also in the outlet pipe immediately below the tank base to homogenise the streamlines. Otherwise the laminar velocity profile would have distorted the concentration determination in the flow-through cells (Ref.11). The concentration in this exit stream could be measured with a relative error of approx. 2% , this being also the error in the RTD density function. The sample volume or "scale of scrutiny" was $1.1 \times 10^{-6} \text{ m}^3$. Input and output signals were plotted and also stored on magnetic tape for computer evaluation.

Fig.2 shows an idealised RTD from which the following times could be estimated:

- a) Dead or breakthrough time t_D ;
- b) Circulation time t_c ;
- c) Mixing time t_m . (time needed for measured RTD to come within 4% of the theoretical value)

t_m was subject to considerable scatter and was to some extent subjectively determined. The density function of the RTD was also Fourier transformed and represented in Bode and Nyquist diagrams, which allowed comparison with the classical analytical forms for a perfectly mixed unit and also the determination of mean residence time \bar{t} and t_c . Integration of the density function over the time in the usual way also gave the mean (\bar{t}) and variance of the RTD.

Various tests were conducted. The helix was replaced by a propeller and eosine - a fluorescent substance - in water was well mixed. Taking absorption signals from the optical cells, the nominal mean residence time (τ) of 346 s was estimated with an error of ± 12 s ($\pm 3.5\%$). Linearity and reproducibility with two fluorescent substances were also established, although the outlet signal was noisy. The larger fluctuations were caused by a few air bubbles and particles of dirt. The smaller ones were due to streaks of concentrated tracer, which are characteristic of coarse-scale, non-turbulent mixing, and noise in the electronics at low absorptions (transmission $> 95\%$).

RESULTS

Power consumption

The ranges of Re numbers covered at the smaller and larger scales were $20-770$ respectively $3400-7700$. The results from the smaller tank covered the end of the laminar region ($Re < 100$) and the start of the transition region, as is shown in Fig.3 for impeller A pumping in both directions. Here, as well as for impellers B, D and G, some $10-15\%$ more power was drawn when pumping upwards. For impellers E and A* there was no effect of direction, while for C and F about 20% less power was consumed pumping upwards; these impellers had the smallest wall clearance. The inverse proportionality between the power and Re numbers ended in all cases at $Re \approx 100$, as found earlier (Ref.6) for Newtonian fluids.

Power measurements in the laminar region may be grouped to account for geometrical variables:

- a) Using the analogy between Couette flow and the shear in the gap between the impeller and the wall (Ref. 3, 6);
- b) An extension of method a) taking into account the surface area of the helix (Ref.12);
- c) Multiple, non-linear regression.

The applicability of method a) is discussed elsewhere (Ref.8), where smooth changes in power consumption with pitch and clearance were found. These may be summarised in the empirical correlation (method c):

$$Po = 134 (h/D) (s/D)^{-0.3} (c/D)^{-0.3} Re^{-1} \quad [1]$$

The width of the helix (w) was not included, since for all 7 impellers w/d was constant (0.12). The measured values of the product $Po.Re$ are given in Table 3.

Equation [1] fitted these values relating to the laminar regime with an average error of 2 %. It should not of course be applied to non-Newtonian fluids and geometries not included in Table 1. The decrease in shear rate and power consumption with increasing pitch and wall clearance, explained previously (Ref.6) using the Couette flow analogy, is also evident in equation [1].

Fig.4 shows on the left hand side power data taken for impeller A from the smaller tank while the 4 points on the right refer to the larger tank (impeller A*). Although these impellers have the same pitch ($s/d = 0.35$), A has the larger clearance ($d/D = 0.908$ compared to 0.954 for A*). Using equation [1] to estimate the power consumption of a smaller impeller with the same clearance as A* ($d/D = 0.954$), the broken line is obtained. Extrapolating this downwards to the Re range in the larger tank, it is clear that the measured power consumption for the larger tank exceeds the extrapolated value by approx. 60 %. The identity of the slopes (approx. -0.72) suggests that the transition region is broad extending from Re 100 to at least 8000. Earlier measurements (Ref.6) using the large tank had also a slope of -0.72 in the transition regime and showed no discontinuity at Re up to 1100. The reason for the rapid increase in power consumption is probably the formation of Taylor vortices between the impeller and the wall. The critical Re for vortex formation when the inner cylinder rotates is (Ref.13):

$$\frac{\Omega_i K R_i^2 \rho}{\mu} = \frac{41.3 K^{5/2}}{(1-K)^{3/2}} \quad [2]$$

where $\Omega_i = 2\pi N$; $K = 0.954$; $R_i = d/2$. Whence $Re_{crit} = (n d^2 \rho/\mu)_{crit} = 2500$. Thus Taylor vortices should have been present in the larger tank over the range of Re covered here (3400-7700). It is known that they increase drag by initially 60-80 % (Ref. 14), which agrees fairly well with the rise shown in Fig. 4.

Batch blending time

The blending time was equal to the decolourisation time. It was multiplied by the stirrer speed to give the dimensionless blending time Nt_m . Values are shown in Fig.5 for both pumping directions with impeller A. The average values of Nt_m for upwards and downwards pumping are 53.0 and 52.9, which are not significantly different. Nt_m has the same value in the laminar ($Re < 100$) as in the transitional region. Impeller A* in the larger tank showed similarly no effect of pumping direction on Nt_m (up 45.7; down 45.2), the average value being 45.5. Thus at Re in the range 3000-8000, Nt_m was 14 % smaller than in the laminar and early transition region, possibly due to more intense secondary flows e.g. in the Taylor vortices. These results confirm the initial studies of Nagata (Ref.1), who found Nt_m to be essentially independent of viscosity.

The corresponding values of Nt_m for all 7 impellers in the smaller tank are given in Table 4, where the effect of pumping direction has been averaged out. Comparing the impellers A, B and C or D, E and F with each other, clearance has little effect on Nt_m . However A, B and C compared to D, E and F (Table 1) shows a somewhat faster mixing for a pitch of approx. 0.57, but then a deterioration if the pitch is further increased to 0.81 (impeller G).

Optimal impeller selection

From all results for smaller tank, it was possible to calculate the specific mixing energy and the specific power consumption of each impeller. The results are presented in Fig.6, where no distinction could be drawn between impellers B and E.

For a given blending time impeller D requires the least energy input. For a given energy input D blends faster e.g. specific energy consumption 40 kJ/m^3 , t_m is 36 s for D and 66 s for A, which is the next fastest impeller. The geometry of helix D is (Table 1):

$$d/D = 0.91$$

$$s/d = 0.57$$

$$h/d = 1.17$$

$$w/d = 0.12$$

which differs significantly from Nagata's optimum (Ref.4). It cannot be decided on the basis of our measurements if a still smaller value of d/D would be even more favourable. This depends on whether the clearance would be reached where the pumping capacity begins to fall drastically, so that despite falling power consumption mixing times and energies would increase rapidly.

In agreement with Nagata's original finding (Ref.1), the specific energy input to attain a given degree of homogeneity falls with increasing mixing time, i.e. with decreasing impeller speed.

Scale-up

In the laminar region it can easily be shown that scale-up with the same geometry at constant power input per unit volume requires constant stirrer speed and results in a constant blending time.

However the constancy of process result (blending time), which as given above will be satisfied by constant N , involves an increase of Re as the square of the impeller (and tank) diameter. The laminar region extends to $Re \approx 100$ and transitional flow within the larger tank becomes probable. In this case, P/V will inevitably be higher on the larger scale. Physically the energy dissipation in the Taylor vortices and other secondary flows is accompanied by a disproportionately small increase in mixing rate. In the experiments reported here (Fig.4), it was found that P/V was 3 - 3.5 times the value required at small scale to give the same blending time. For example $t_m = 40 \text{ s}$ required 0.2 kW m^{-3} and 0.6 kW m^{-3} at small and large scale respectively. Keeping 0.2 kW m^{-3} at large scale would have extended t_m to 70 s.

Continuous operation

Form of the RTD:

Irrespective of pumping speed and direction and of throughput, all RTD curves consisted first of a dead time, then some irregular fluctuations and finally an exponentially falling section (Fig.2). A summary of the most important results is presented here, further details being available elsewhere (Ref.10).

Dead time t_p :

This consisted of two transport lags - one in each of the feed and product pipes - together with a transport time within the tank, as tracer followed a laminar path from inlet to outlet. The total length of the pipes was 0.2 m and the transport lag rose from 1 to 7 s as the throughput decreased and the nominal mean residence time (τ) increased from 198 to 1390 s.

In the laminar region (viscosity 1.0 Pa s ; $Re = 55$; $N = 40 \text{ rpm}$), the dead time in the mixer itself depended strongly on the pumping direction (Fig.7). At the minimum and maximum mean residence times, these dead times were 27 s (up), 3 s (down) respectively 35 s (up) and 8 s (down). As shown in Fig.8, these dead times are consistent with the length of the paths from inlet to outlet. The primary circulation in one pumping direction is presumably simply the reverse of that in the other direction, so that the sum of the dead times should equal the circulation time. For example with nominal mean residence times of 347 and 462 s, dead times were 27 s (up) and 4 s (down) respectively 29 s (up) and 4 s (down). These values estimate the circulation times as 31 s respectively 33 s; measured circulation times averaged over the two pumping directions

were 29 s respectively 33 s.

t_D decreases only slightly with rising throughput. This may be interpreted by comparing the circulation rate in the tank at zero throughput Q with the throughput q . Q is estimated from $Q \approx 0.06 Nd^3$. This gives $Q \approx 0.73 \text{ dm}^3 \text{ s}^{-1}$, while q ranged from 0.02 to $0.12 \text{ dm}^3 \text{ s}^{-1}$. Since q is at most 16 % of the pumped flow, a maximum decrease of 16 % of t_D (6 s up, 1 s down) would be anticipated.

t_D depended also on N . Over the range 20-100 rpm, the following regressions resulted:

$$t_D(\text{down}) = 3.1 N^{-0.72} \quad t_D(\text{up}) = 21 N^{-0.66} \quad [3]$$

for $347 < \tau < 462 \text{ s}$.

When operating with downwards pumping, very short breakthrough times and therefore short circuiting could be avoided by simply interchanging the inlet and outlet positions used here, thus increasing the liquid path.

Circulation time (t_c) and pumping capacity (Q):

For the reasons given above, a reduction of at most 4 s in t_c as q rose to its maximum value was anticipated. Because this is within the limits to which t_c can be determined, the effect of q on t_c will be neglected. Identifying t_c by the peaks of the Bode diagramme at various speeds gave the following regressions:

$$t_c(\text{down}) = 18 N^{-1.02} \quad t_c(\text{up}) = 22 N^{-0.99} \quad [4]$$

$$\text{Average: } Nt_c = 20$$

The pumping capacity follows immediately if it may be assumed that no dead zones are present, so that the whole volume divided by t_c is Q . Hence, using the average:

$$Q = 0.065 Nd^3 \quad (\text{pitch } s/d = 0.57) \quad [5]$$

The constant in this result is consistent with 0.046 (Ref.3) for a pitch of 0.35 and 0.083 [impellers I and VI (Ref.15)] for a pitch of 0.69-0.72.

Mixing time (t_m):

This was estimated subjectively as the time which elapsed before the initial oscillations were fully damped and before the residence time curve decreased exponentially. Values of t_m scattered considerably, did not vary significantly with q , but were multiples (3.0 to 3.5) of t_c , i.e. 3 to 3.5 circulations suffice to homogenise the tank contents. Very similar results have been obtained earlier (Ref.1, 15).

Combining this result with equation [4] suggests that $Nt_m \approx 65$. This predicts slower mixing than the result given in Table 4: $Nt_m = 50$ for batch blending with impeller D. However a fast reaction with 40 % excess of reagent was then used, whereas here only the blending of a dyestuff has been characterised (this might be better compared to a reaction with stoichiometric quantities of reagents and Table 2 suggests that Nt_m would have been 58 and not 50; this is still faster than $Nt_m \approx 65$, probably because of the steepened concentration gradients and faster diffusion when using a neutralisation).

Influence of Re and viscosity:

All results presented above refer to the laminar flow region ($Re < \text{approx. } 100$). By diluting and/or warming the glycerine, the range of Re was extended to 560. t_c remained inversely proportional to N over the whole range of Re and circulation was again 20 % faster when pumping downwards. Nt_c was given by equation [4] (Fig.9), indicating no effect of Re in the early transition region.

The mixing times followed the circulation times in the transition region and $t_m \approx 3 t_c$. Thus, as in the batch neutralisations reported above, no reduction in Nt_m on moving into the transition region occurred. Exceptionally long mixing times in the transition region (Ref.16) were not observed using either neutralisation or dye distribution.

Mean residence time (\bar{t}):

The nominal mean residence time (V/q) was compared to the mean value determined from the residence time distribution. This determination requires integration of the density function of the RTD over the time and during t_m this function oscillates rapidly depending upon the pumping direction as pulses of almost undiluted tracer leave the tank. This introduces some inaccuracy into the numerical integration, because although $t_m < \bar{t}$ (e.g. 100 s and 400 s) the integrand is largest at the start.

Fig.10 shows, for a nominal mean residence time of 346 s, how the value \bar{t} determined from the RTD depended on N . With upwards pumping, \bar{t} decreased by up to 19 % of τ and this may be understood by examining the secondary flow loop (Fig.8). This was driven by the axial variation of the radial pressure gradient ($\partial P/\partial r = \rho r \omega^2$) as ω falls to zero on the tank base (Ref.3). This flow caused a short circuit at a rate which rose as N increased, and so reduced the actual mean residence time. With downwards pumping the increase of \bar{t} above 346 s (up to 14 %) was probably caused by weakly agitated zones near the corners of the base, which become larger when pumping down, and possibly also near the shaft. Such zones take up tracer from faster flowing fluid when its concentration is high and release it later, thus increasing \bar{t} . This effect is characteristic of a flow which is highly non-uniform.

CONCLUSIONS

- 1) Power measurements for Newtonian fluids covering the range $20 < Re < 7700$ showed an unexpected increase in the power number of about 60 % well into the transitional region (Fig.4). The values of Re where this increase was measured and also the magnitude of the increase were consistent with the formation of Taylor vortices between the helix and the wall. The dimensionless blending time decreased by 14 % pointing to a small contribution from the vortices to mixing.
- 2) The influences of wall clearance and pitch on the power consumption in the laminar region (Table 3) have been correlated empirically in equation [1]. Considering simultaneously power and blending times (Table 4), impeller D has been shown (Fig. 6) to consume the least energy in blending Newtonian liquids within a given time. A still higher wall clearance ($> 0.05 D$) might result in a further energy saving without loss of pumping capacity.
- 3) Power consumption and blending time were measured at two scales (0.023 and 0.73 m^3). Scaling-up at constant impeller rotational speed is likely to increase Re such that transitional flow exists at large scale, whereas laminar flow existed at small scale. The consequence would then be a slight reduction of blending time, but a substantial increase in power consumption per unit volume at large scale.
- 4) Residence time distribution measurements, using photometric determination of the concentration of a photochromic dye, showed more noise than was desirable. Some of this could be attributed to technical problems (air bubbles, dust particles, electronic noise at low absorptions and therefore high amplifications), some was however probably the consequence of the coarse scale after laminar flow mixing, whereby streaks of concentrated dye passed through the sample volume.
- 5) The breakthrough time (Fig.7) was obviously related to the pumping direction and the position of the inlet and outlet (Fig.8). It decreased with rising stirrer speed [equation 3]. The dimensionless circulation time Nt_c depended little on Re [equation 4] (Fig.9). Mixing was accomplished in about 3 circulations. The circulation capacity of the impeller was given by $Q = 0.059 Nd^3$ (upwards pumping) and $0.072 Nd^3$ (downwards pumping), indicating the role of secondary flow (Fig.8). The measured mean residence time deviated from its nominal value by up to -19 % (upwards pumping) and +14 % (downwards pumping). After the initial transients due to the circulation of only weakly mixed tracer had passed, the residence time distribution at the lower stirrer speeds (20-50 rpm) was well described by the ideal mixing model [this conclusion was drawn after representing the RTD on Bode and Nyquist plots (Ref.10)].

REFERENCES

- 1) Nagata S., Yanigimoto M. and Yokoyama T. "A study on the mixing of high-viscosity liquid". J.Chem.Eng.(Japan) 21, 278 (1957).
- 2) Metzner A.B. and Taylor J.S. "Flow patterns in agitated vessels". AIChE.J. 6, 109 (1960).
- 3) Bourne J.R. and Butler H. in "Mixing - Theory related to Practice". Ed. Rottenburg P.A., London, Inst.Chem.Engrs., p.89 (1965).
Bourne J.R. and Butler H. "An analysis of the flow produced by helical ribbon impellers". Trans.Inst.Chem.Eng. 47, T-11 (1969).
- 4) Nagata S. "Mixing - Principles and Applications". Kodansha Ltd./Wiley, Tokyo (1975).
- 5) Harada M., Tanaka K., Eguchi W. and Nagata S. "The effect of micro-mixing on the homogeneous polymerization of styrene in a continuous flow reactor". J.Chem.Eng. (Japan) 1, 148 (1968).
- 6) Bourne J.R. and Butler H. "Power consumption of helical ribbon impellers in viscous liquids". Trans.Inst.Chem.Engrs. 47, T-263 (1969).
- 7) Ford D.E., Mashelkar R.A. and Ulbrecht J. "Mixing times in Newtonian and non-Newtonian fluids". Process Tech.Internat. 17/10, 803 (1972).
- 8) Knoepfli W. "Charakteristik eines Wendelrührers beim Mischen viskoser Newton'scher Flüssigkeiten unter Berücksichtigung des Einflusses der Rührergeometrie auf die Leistungsaufnahme und die Mischzeit". Dissertation No. 5105, ETH Zurich (1973) (in German).
- 9) Bourne J.R., Giger G.K., Richarz W. and Riesen R. "A photochromic tracer system for residence time measurements in highly viscous fluids". Chem.Eng.J. 12, 159 (1976).
- 10) Riesen R. "Charakteristik eines Wendelrührers beim kontinuierlichen Mischen einer hochviskosen Newton'schen Flüssigkeit". Dissertation No. 6171, ETH Zurich (1978) (in German).
- 11) Levenspiel O. and Turner J.R.C. "The interpretation of residence-time experiments". Chem.Eng.Sci. 25, 1605 (1970).
- 12) Chavan V.V. and Ulbrecht J. "Power correlation for helical ribbon impellers in inelastic non-Newtonian fluids". Chem.Eng.J. 3, 308 (1972).
- 13) Bird R.B., Stewart W.E. and Lightfoot E.N. "Transport Phenomena", p.96. Wiley, New York (1960).
- 14) Schlichting H. "Boundary-Layer Theory", p.503. McGraw-Hill, New York (1968).
- 15) Carreau P.J., Patterson I. and Yap C.Y. "Mixing of viscoelastic fluids with helical ribbon agitators. I: Mixing time and flow patterns". Can.J.Chem.Eng. 54, 135 (1976).
- 16) Zlokarnik M. "Eignung von Rührern zum Homogenisieren von Flüssigkeitsgemischen". Chem.Ing.Tech. 39, 539 (1967)(in German).

Table 1: Geometries of helical ribbon impellers.

Impeller	d/D	s/D	h/D	w/D	z _o /D
A	0.908	0.354	1.082	0.111	1.243
B	0.971	0.352	1.082	0.107	1.243
C	0.986	0.345	1.066	0.108	1.225
D	0.907	0.518	1.065	0.110	1.229
E	0.974	0.523	1.065	0.110	1.229
F	0.988	0.510	1.049	0.108	1.211
G	0.894	0.726	1.131	0.111	1.229
A*	0.954	0.345	1.060	0.104	1.220

Table 2: Blending times and acid/base ratios.

Impeller	H ₂ SO ₄ /NaOH:	1	1.2	1.4	1.6
A	Blending time (s):	67	61	56	55
D		58	52	51	50

Table 3: Measured values of PoRe in the laminar regime.

Impeller:	A	B	C	D	E	F	G
Po Re:	530	720	932	407	639	800	402

Table 4: Measured average values of Nt_m.

Impeller:	A	B	C	D	E	F	G	A*
Nt _m (s):	53	56	60	50	49	54	88	45

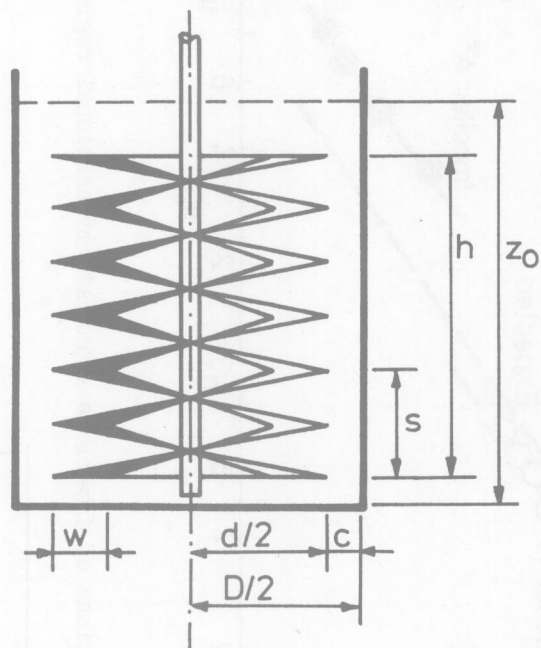


Fig. 1 The helical ribbon impeller.

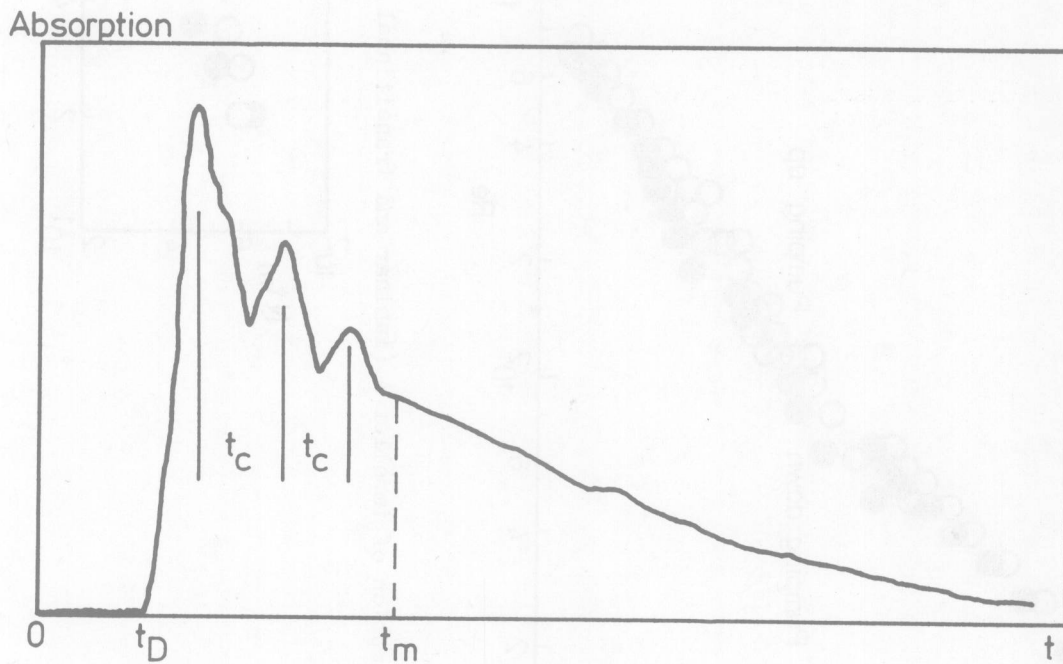


Fig. 2 The form of the residence time distribution.